Inhibition of Ras-guanine nucleotide-releasing factor 1 (Ras-GRF1) signaling in the striatum reverts motor symptoms associated with L-dopa–induced dyskinesia

Stefania Fasano[a,b,1], Erwan Bezard[c,d,1], Angela D'Antoni[b], Veronica Francardo[a], Marzia Indrigo[b], Li Qin[d], Sandra Doveró[c], Milica Cerovic[e], M. Angela Cenci[a,2], and Riccardo Brambilla[b,e,2,3]

[a]Basal Ganglia Pathophysiology Unit, Department of Experimental Medical Science, Lund University, BMC F11, Lund 221 84, Sweden; [b]Division of Neuroscience, Institute of Experimental Neurology, San Raffaele Scientific Institute, 20132 Milan, Italy; [c]Université Victor Segalen-Bordeaux 2, Centre National de la Recherche Scientifique, Institute of Neurodegenerative Diseases, 33076 Bordeaux, France; [d]Institute of Laboratory Animal Sciences, China Academy of Medical Sciences, 100050 Beijing, China; and [e]School of Biosciences, Cardiff University, Cardiff CF10 3AX, United Kingdom

L-dopa–induced dyskinesia (LID) is a common debilitating complication of dopamine replacement therapy in Parkinson's disease. Recent evidence suggests that LID may be linked causally to a hyperactivation of the Ras–ERK signaling cascade in the basal ganglia. We set out to determine whether specific targeting of Ras-guanine nucleotide-releasing factor 1 (Ras-GRF1), a brain-specific activator of the Ras–ERK pathway, may provide a therapy for LID. On the rodent abnormal involuntary movements scale, Ras-GRF1–deficient mice were significantly resistant to the development of dyskinesia during chronic L-dopa treatment. Furthermore, in a nonhuman primate model of LID, lentiviral vectors expressing dominant negative forms of Ras-GRF1 caused a dramatic reversion of dyskinesia severity leaving intact the therapeutic effect of L-dopa. These data reveal the central role of Ras-GRF1 in governing striatal adaptations to dopamine replacement therapy and validate a viable treatment for LID based on intracellular signaling modulation.

Parkinson's disease (PD) is a neurodegenerative disorder characterized by a loss of dopaminergic neurons in the substantia nigra pars compacta (SNc) causing dopamine depletion in the striatum, the main input nucleus of the basal ganglia. Dopamine replacement therapy with L-dopa remains the most effective treatment for PD, but its use is associated with motor fluctuations and abnormal involuntary movements (AIMs), termed "L-dopa–induced dyskinesia" (LID), which are dose-limiting and potentially disabling (1–3).

A key objective for the future treatment of PD is to avoid dyskinesia altogether, but doing so will require an understanding of the molecular mechanisms that are involved. LID is attributed to a sequence of events, largely occurring in the striatum, that include pulsatile stimulation of dopamine D1 receptors, downstream changes in proteins and genes, dendritic alterations, and functional abnormalities in nondopaminergic transmitter systems, all of which concur to modify neuronal firing patterns in the basal ganglia–thalamocortical networks (1–4). Once symptoms have appeared, LID can be triggered easily by a single dose of L-dopa even after several weeks of treatment washout (4). Regulation of striatal gene expression is the likely mechanism underlying neuronal plasticity in LID. The ERK signaling cascade is a key regulator of striatal plasticity and an interesting candidate for drug targeting (5–8). Stimulation of dopamine and glutamate receptors on striatal neurons can switch on the small GTPases of the Ras family, which in turn activate the Raf/Mek/Erk protein kinase cascade (5–8). Sustained activation of these biochemical pathways leads to synaptic rearrangements requiring de novo gene expression and protein synthesis. Importantly, in neurotoxic models of PD, such as the unilaterally 6-hydroxydopamine (6-OHDA)-lesioned rodent and the 1-methyl-4-phenyl-1,2,3,6-tetrahydropyridine (MPTP)-treated nonhuman primate (NHP), a supersensitivity of striatal D1 receptors leads to ERK hyperactivation in response to L-dopa, and this response

correlates positively with LID severity (9–11). Moreover, inhibition of this pathway with systemically active drugs has been proposed recently as a treatment for LID (10, 12).

However, this evolutionarily conserved signaling cassette is involved in a number of important cellular responses, including memory formation and synaptic plasticity in the CNS and cell proliferation and survival in most cell types (5, 13–17). This involvement raises concerns about the validity of therapeutic interventions based on systemic inhibition of the Ras–ERK pathway. However, such concerns could be overcome by reducing, rather than blocking, Ras–ERK activation exclusively in the motor part of the striatum, the region of the brain most directly implicated in LID. In addition, a safe therapy for LID would have to target components of the Ras–ERK pathway that are not implicated in cell survival. To achieve such goals, we have addressed the potential involvement in LID of the neuron-specific Ras–guanine nucleotide-releasing factor 1 (Ras-GRF1), which catalyzes the conversion of Ras from an inactive GDP-bound form to an active GTP-bound form (5). We recently demonstrated that this molecule plays a crucial role in the regulation of ERK-mediated cellular and behavioral responses to psychostimulants by sensing and integrating dopamine and glutamate signals in striatal neurons (18). Ablation of Ras-GRF1 in the mouse abrogates the ability of glutamate and D1 receptor agonists to activate the ERK pathway, leaving intact the responses to survival factors such as BDNF. Accordingly, the loss of Ras-GRF1 reduces the rewarding and locomotion-inducing properties of cocaine, along with the activation of ERK in striatal neurons (18).

Because the behavioral and cellular responses to psychostimulants and L-dopa share some molecular similarities, we set out to investigate the role of Ras-GRF1 in LID.

Results

Ras-GRF1 Ablation Reduces AIMs in the Murine Model of LID. We first generated a 6-OHDA–based model of PD and LID in Ras-GRF1–deficient mice (Ras-GRF1–KO) (19). The neurotoxin was injected into the right medial forebrain bundle in both Ras-GRF1–KO mice and WT littermates. A test of spontaneous ipsilateral rotation 2 wk after surgery showed a similar degree of rotational

asymmetry in the two genotypes, suggesting an equivalent sensitivity to the neurotoxic damage (Fig. 1A). This evidence was later confirmed using tyrosine hydroxylase (TH) immunohistochemistry, which revealed more than 90% depletion of striatal dopamine fiber terminals and nigral dopamine cell bodies in both groups (Fig. S1 A–H).

To elicit axial, limb, and orolingual AIMs, we applied an ascending-dose regimen of L-dopa (1.5, 3, 6 mg/kg, twice daily for 9 consecutive days) to both 6-OHDA–lesioned WT and Ras-GRF1 mutant animals. We set up this protocol to detect subtle differences between genotypes in the sensitivity to L-dopa that may have been masked by the use of higher drug doses (20, 21). Daily scoring of AIMs revealed a gradual development of dyskinesia in both genotypes. However, for all doses of L-dopa, the AIMs scores were significantly lower in Ras-GRF1–KO mice than in their littermate controls (Fig. 1B). Remarkably, Ras-GRF1 ablation did not affect locomotive AIMs (Fig. 1C). These results demonstrate that the absence of Ras-GRF1 strongly attenuates LID induction in mice without compromising the motor stimulant effect of L-dopa. Consistently with previous experimental evidence (9–11, 22), we observed abnormally high levels of ERK1/2 phosphorylation and FosB/ΔFosB immunoreactivity in the dorsolateral lesioned striatum of WT mice. In marked contrast, much lower levels of ERK1/2 phosphorylation and FosB/ΔFosB expression were observed in the Ras-GRF1 mutants (Fig. 1 D and E and Fig. S2 A and B).

Pharmacogenetic Interaction Between Ras-GRF1 and ERK1/2 Blockade. Because AIMs expression in Ras-GRF1 mutant mice was only attenuated, not completely abolished, we next explored the possibility of a pharmacogenetic interaction between Ras-GRF1 loss and a direct chemical inhibition of the core component of the ERK signaling pathway. Systemic administration of high doses (>50 mg/kg) of SL327, a specific chemical inhibitor of the ERK upstream kinase MEK1/2, already has been shown to inhibit ERK signaling in the striatum efficiently (10, 23). Using 6-OHDA–lesioned drug-naive mice, we first evaluated the effects of three different doses of SL327 (10, 30, and 50 mg/kg, i.p.) on the cellular and behavioral responses to an acute L-dopa challenge. Only the lowest dose of SL327 (10 mg/kg) was found to alter neither L-dopa–induced contralateral turning behavior nor the striatal expression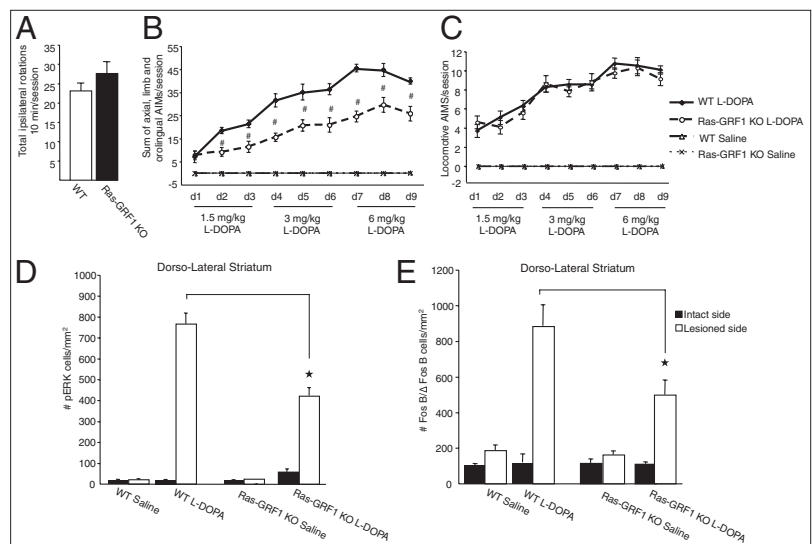 of phosphorylated ERK1/2 and FosB/ ΔFosB (Fig. S3 A–C). We next asked whether this normally ineffective dose of SL327 may cause a further reduction of the AIMs in a Ras-GRF1–deficient genetic background.

Hemiparkinsonian Ras-GRF1–KO and control mice were pretreated with 10 mg/kg of SL327 and injected 30 min later with L-dopa (1.5, 3, and 6 mg/kg, the same escalating regimen as above). As expected, SL327 did not change the dyskinesia profile in control animals but greatly attenuated the AIMs scores in Ras-GRF1 mutants (Fig. 2A). Importantly, Ras-GRF1 ablation and SL327 treatment did not affect locomotive AIMs or contralateral turning behavior, indicating that L-dopa–induced motor activation is not diminished by the pharmacogenetic intervention (Fig. 2 B and C). The reduction in AIM scores was paralleled by a significant inhibition of phosphorylated ERK1/2 (pERK1/2) and FosB/ΔFosB expression by SL327 in the Ras-GRF1–KO group (Fig. 2 D–F).

Postsynaptic changes in striatal medium spiny neurons (MSNs) following dopamine depletion and chronic L-dopa administration play a key role in the development of LID. In particular, recent evidence indicates that LID results from a supersensitivity of D1 receptors, which are expressed preferentially in the striatonigral MSN population, leading to a selective hyperactivation of ERK signaling in these cells (24). By using two types of BAC-transgenic mice expressing EGFP specifically in striatonigral or striatopallidal MSN [namely, M4-EGFP mice (striatonigral neurons, direct pathway) and adenosine receptor A2A-EGFP mice (striatopallidal neurons, indirect pathway)], we addressed the cellular localization of Ras-GRF1 in the striatum. A Ras-GRF1–positive signal was found in EGFP-labeled neurons in both mouse lines (Fig. 3 A and C). Quantitative dual-fluorescence confocal analysis indicated that Ras-GRF1 was expressed equally in both pathways (53.6% in the direct pathway; 46.4% in the indirect pathway) (Fig. 3E). As expected, Ras-GRF1 expression was absent in both M4-EGFP/Ras-GRF1–KO and A2A-EGFP/Ras-GRF1–KO double mutants (Fig. 3 B and D). These data indicate that the specific involvement of Ras-GRF1 in LID is not caused by a selective expression of this factor in striatonigral MSN but rather reflects its specific engagement by D1 receptors.
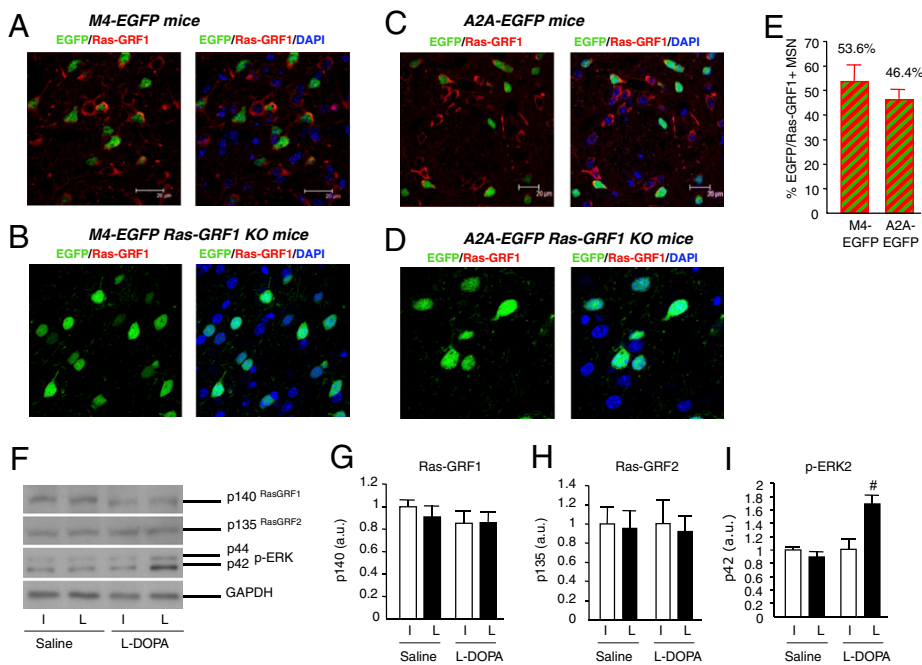
In addition to D1 receptors, other key signaling molecules show altered levels of expression in LID (25, 26). Interestingly, a recent study has shown that two striatally enriched regulators of Ras–ERK signaling, CalDAG-GEF 1 and 2, are inversely

Fig. 1. Attenuated AIMs and striatal cellular responses in Ras-GRF1–KO mice after L-dopa treatment. (A) The success of the lesion was evaluated 2 wk after 6-OHDA injection by counting spontaneous ipsilateral rotations in a squared open arena over a 10-min session. WT (n = 16) and mutants (n = 16) displayed an equivalent turning score. (B) Temporal profile of axial, limb, and orolingual AIMs induced by an increasing L-dopa regimen (1.5, 3, and 6 mg/kg, twice a day) administered for 9 consecutive days. The AIM scores were reduced significantly in Ras-GRF1–KO mice (Ras-GRF1–KO L-dopa, dashed line, open circles, n = 9) in comparison with their littermate controls (WT L-dopa, solid line, closed circles, n = 9). Saline treatment (dashed and dotted line marked "x") did not induce involuntary movements (Ras-GRF1–KO saline, n = 7; WT saline, n = 7). Repeated measures and post hoc Tukey's honestly significant difference (HSD) tests showed a genotype effect (#P < 0.001) and a genotype–time interaction effect (P < 0.001). (C) No difference in the locomotive AIMs in WT and Ras-GRF1–KO animals were found in response to L-dopa. (D) Abnormal levels of pERK activation were observed in dyskinetic WT animals, whereas a pronounced reduction was seen in Ras-GRF1–KO animals. The total number of pERK-immunopositive cells/mm² was counted in the dorsolateral striatum (intact and lesion sides) in saline- and L-dopa–treated groups. Two-way ANOVA followed by a Tukey's HSD test indicated a significant genotype difference between WT and Ras-GRF1–KO lesioned lateral striatum (*P < 0.0001). (E) FosB/ΔFosB expression is severely attenuated in the lesioned striata of Ras-GRF1–KO animals (black bars) in comparison with littermate controls (white bars). The total number of FosB/ΔFosB-positive cells/mm² was counted in the dorsolateral striatum of all experimental groups. Two-way ANOVA followed by Tukey's HSD test showed a significant genotype difference between WT mice and Ras-GRF1–KO mice treated with L-dopa (*P < 0.0001 difference).

Fig. 2. Treatment of Ras-GRF1–KO mice with a normally ineffective dose of SL327 caused a further reduction of the AIMs. (*A*) Sum of axial, limb, and orolingual scores (ALO AIMs) after 9 d of escalating doses of L-dopa expressed as means of 3-d doses showed a stronger attenuation of dyskinesia in Ras-GRF1–KO animals pretreated with a low dose (10 mg/kg, i.p.) of SL327 (hatched bars) than in Ras-GRF1–KO mice treated with L-dopa only (black bars). Repeated measures and post hoc Tukey's HSD test: #$P < 0.001$ WT L-dopa (white bar, $n = 10$) vs. Ras-GRF1–KO L-dopa ($n = 9$); ☆$P < 0.01$ Ras-GRF1–KO L-dopa vs. Ras-GRF1–KO SL327 + L-dopa ($n = 10$). (*B*) Locomotive AIMs expressed as means of 3-d doses were not affected by Ras-GRF1 ablation and SL327 treatment. (*C*) Total numbers of contralateral turns (mean ± SEM) induced by L-dopa were comparable among groups. (*D*) Representative photomicrographs of pERK1/2 immunoreactive cells (*Upper*) and FosB/ΔFosB expression (*Lower*) in the dorsolateral part of the striatum after 9 d of L-dopa treatment in combination with SL327 (10 mg/kg). (*E*) Quantification of pERK1/2-positive cells (mean ± SEM) in the intact and lesioned dorsolateral striatum of Ras-GRF1 mutants and control animals. Two-way ANOVA revealed a significant reduction (genotype effect) in the number of pERK-positive cells in lesioned striatum of Ras-GRF1 mutants in comparison with littermate controls (Tukey's HSD test, #$P < 0.001$) and a greater treatment effect in lesioned striatum of Ras-GRF1–KO mice pretreated with SL327 (Tukey's HSD test, ☆$P < 0.001$). (*F*) Quantification of FosB/ΔFosB-positive cells (mean ± SEM) in the intact and lesioned striata of Ras-GRF1–KO mice. Two-way ANOVA showed significant differences (genotype effect) between WT mice and Ras-GRF1–KO mice treated with L-dopa (Tukey's HSD test, #$P < 0.001$). A significant reduction in the number of FosB//ΔFosB immunoreactive cells (treatment effect) also was observed in Ras-GRF1–KO mice treated with SL327 in comparison with Ras-GRF1–KO mice injected with L-dopa only (Tukey's HSD test, ☆$P < 0.001$).

affected in a rat model of LID (27). To determine whether Ras-GRF1 and its close homolog Ras-GRF2 show similar alterations, we examined the levels of these proteins (p140$^{Ras-GRF1}$ and p135$^{Ras-GRF2}$) in the mouse striata by Western blot analysis (Fig. 3*F*). Unlike what was reported for CalDAG-GEFs, the striatal levels of Ras-GRF1/2 did not change in L-dopa–treated dyskinetic animals relative to saline-treated controls, although, as expected, ERK1/2 phosphorylation was significantly up-regulated in the former group (Fig. 3 *G–I*). These data are important because they indicate that Ras-GRF1/2 levels are not regulated by the pathophysiological process at the basis of LID; such regulation could have posed significant problems for a potential therapy targeting this molecule.

Reversion of LID in an NHP Model by a Combined Genetic Inhibition of Ras-GRF1 and ERK. The data above indicate that the absence of Ras-GRF1 in the brain significantly attenuates LID and the associated molecular and cellular abnormalities in the mouse. In an effort to translate these findings into a clinically relevant therapy, we set out to determine (*i*) whether a partial inhibition of Ras-

GRF1 in the striatum can revert already established dyskinesias and (*ii*) whether the therapeutic effect also can be seen in an animal model that better recapitulates the human condition.

Thus, we generated lentiviral vectors (LV) that express two dominant-negative constructs for Ras-GRF1 under the control of the strong and ubiquitous human phosphoglycerol kinase (PGK) promoter in addition to the GFP marker (28, 29). These two constructs were designed using the human sequence of Ras-GRF1 and were tested in the mouse striatum (Fig. S4 *A and B*). The first construct expresses the binding domain of Ras-GRF1 on the NR2B subunit of the NMDA receptor (Ras-GRF1-NR2B-BD), thus specifically blocking glutamate-mediated activation of Ras-GRF1 but not other Ras exchange factors such as the closely related homolog Ras-GRF2 (30). The second dominant-negative construct is a point mutation in the catalytic domain of Ras-GRF1 (Ras-GRF1-CD^{W1056E}), which sequesters Ras proteins and thus blocks the activity of the endogenous Ras-GRF1 without affecting Ras-GRF1–independent ERK activation (31). Expression of both constructs at a high level [∼5 × 10^{10} transforming units (TU)/mL, 1-μL injection per striatum]

Fasano et al.

A M4-EGFP mice
EGFP/Ras-GRF1   EGFP/Ras-GRF1/DAPI

B M4-EGFP Ras-GRF1 KO mice
EGFP/Ras-GRF1   EGFP/Ras-GRF1/DAPI

C A2A-EGFP mice
EGFP/Ras-GRF1   EGFP/Ras-GRF1/DAPI

D A2A-EGFP Ras-GRF1 KO mice
EGFP/Ras-GRF1   EGFP/Ras-GRF1/DAPI

E
% EGFP/Ras-GRF1+ MSN
53.6%   46.4%
M4-EGFP   A2A-EGFP

F
p140 $^{Ras-GRF1}$
p135 $^{Ras-GRF2}$
p44
p42 p-ERK
GAPDH
I L   I L
Saline   L-DOPA

G Ras-GRF1
p140 (a.u.)
I L I L
Saline L-DOPA

H Ras-GRF2
p135 (a.u.)
I L I L
Saline L-DOPA

I p-ERK2
p42 (a.u.)
#
I L I L
Saline L-DOPA

Fig. 3. Expression of Ras-GRF1 in MSN subpopulations and its protein levels in dyskinetic animals. Immunofluorescence of Ras-GRF1 (red), EGFP (green), and nuclear labeling with DAPI (blue) of striatonigral neurons (direct pathway) of M4-EGFP mice (A) and striatopallidal neurons (indirect pathway) of A2A-EGFP mice (C). (Scale bars in A and C: 20 μm.) (E) The graph shows the percentage of the total Ras-GRF1–positive neurons that are GFP-positive, indicating that Ras-GRF1 is expressed equally in each subpopulation. As expected, Ras-GRF1 was not expressed either in the direct pathway of M4-EGFP Ras-GRF1–KO mice (B) or in the indirect pathway of A2A EGFP Ras-GRF1–KO mice (D). (F) Protein levels of Ras-GRF1, Ras-GRF2, and pERK1/2 in intact (I) and lesioned (L) striata of WT mice after 9 d of L-dopa treatment were determined by Western blot analysis. p140 $^{Ras-GRF1}$ (G) and p135 $^{Ras-GRF2}$ (H) levels were not altered in dopamine-denervated striata after saline or L-dopa treatment, whereas phosphorylation of ERK1/2 is enhanced only in L-dopa–treated striata (I) (one-way ANOVA, #$P < 0.01$).

showed a significant inhibitory effect on the ability of 20 mg/kg cocaine to activate ERK1/2. We next investigated whether the effect mediated by Ras-GRF1 inhibition can be enhanced further by a concomitant suboptimal manipulation of the core MEK–ERK component of the pathway. To this end we tested the ability of a dominant-negative mutant of ERK2, ERK2^{K52R}, to attenuate ERK activation in this system (32). A high titer of LV-ERK2^{K52R} ($\sim$5 × 10^{10} TU/mL) was capable of reducing ERK1/2 phosphorylation in response to cocaine, whereas a lower titer ($<1 \times 10^{10}$ TU/mL) was ineffective. Interestingly, a significant reduction of pERK1/2 levels was obtained using a mix of the three LV containing high titers of the two LV-Ras-GRF1 constructs and a low titer of LV-ERK2^{K52R} (LV-Mix-GFP; 1:1:1).

We next investigated the effectiveness of the LV-Mix-GFP in the "gold standard" experimental model of LID, the MPTP-lesioned L-dopa–treated macaque monkey. The decision to use LV-Mix-GFP instead of individual vectors was justified by both the lack of knowledge about the effect of these constructs in the primate and a need to minimize the use of animals. Six L-dopa–treated dyskinetic macaques received the control LV-GFP ($n = 3$) or the therapeutic LV-Mix-GFP vectors ($n = 3$) in the motor striatum. Upon completion of the behavioral experiments, all monkeys were tested to determine the extent of the lesion (Fig. S5A) and transduction efficacy (Fig. S5 B and C). Both groups had a similarly extensive nigrostriatal cell loss, as evidenced by a dramatic decrease in the number of TH-immunopositive neurons in the SNc.

Before LV administration, parkinsonian disability scores in both the OFF (before L-dopa administration) and ON states (after L-dopa administration), LID scores in the ON state, and the time course of L-dopa–induced locomotor activity were indistinguishable between the two groups. Starting at 8 wk postsurgery, when behavioral experiments resumed, the antiparkinsonian efficacy of L-dopa remained intact in the LV-Mix-GFP group compared with LV-GFP animals (Fig. 4 A and B). However, monkeys expressing the LV-Mix-GFP had significantly less severe LID (Fig. 4 C and D) and a significant decrease in L-dopa–induced locomotor hyperactivity during the ON state (Fig. 4 E and F). The latter effect is consistent with an antidyskinetic action of the vector therapy, because high locomotor counts ON L-dopa are associated with LID and reflect excessive motor activation. Taken together, these results indicate that striatal expression of the two dominant-negative Ras-GRF1 proteins associated with a low titer of dominant-negative ERK2 construct diminishes LID severity without reducing the positive effects of L-dopa on parkinsonian motor scores.

Because L-dopa therapy activates both D1 and D2 receptors, we next investigated how the expression of the dominant-negative constructs modifies responses to D1 and D2 agonists. Administration of a D1 agonist produced a similar amelioration of parkinsonian features in all animals (Fig. 4 G and H), but the severity and duration of dyskinesia were reduced significantly in the LV-Mix-GFP group compared with the LV-GFP controls (Fig. 4I). In contrast, the antiparkinsonian and prodyskinetic effects of a D2 agonist did not differ between the two groups (Fig. 4 I and J). These data suggest that the antidyskinetic action of the LV-Mix-GFP vectors is mediated through striatal neurons expressing the D1 receptor.

A comparable extent of LV transduction, covering the entire motor putamen, was observed in the LV-GFP and LV-Mix-GFP groups. However, the LV-Mix-GFP group showed a dramatic reduction in the number of pERK- and FosB/ΔFosB-immunopositive striatal neurons following L-dopa treatment (Fig. S5 D and G).

Discussion

Dyskinesia remains a major therapeutic problem in PD. Currently, the only marketed drug available to treat LID is amantadine, a weak NMDA antagonist that can produce psychotic side effects and usually provides a short-lasting benefit (33). Attempts to control LID symptoms by targeting serotonergic or glutamatergic systems have been successful at the experimental level but have produced variable results in clinical trials (34). The recent understanding that LID is essentially caused by a dysregulation of D1 receptor-mediated intracellular signaling in the striatum opens perspectives for innovative treatments (9–11, 21, 35, 36). Pharmacological antagonism of D1 receptors is not a viable option, because it would compromise the therapeutic action of L-dopa. In contrast, partial inhibition of hyperactive signaling pathways downstream of the D1 receptor would target long-term maladaptive neuroplasticity specifically without reducing the positive effects of dopamine replacement therapy. The Ras–ERK pathway appears to be the target of choice for such an approach, because its hyperactivity causes abnormal striatal plasticity in LID (37). Unfortunately, a global inhibition of the ubiquitously expressed Ras-Raf-MEK-ERK cascade may interfere with cell-survival mechanisms downstream of growth factor receptors (5). Restricting such
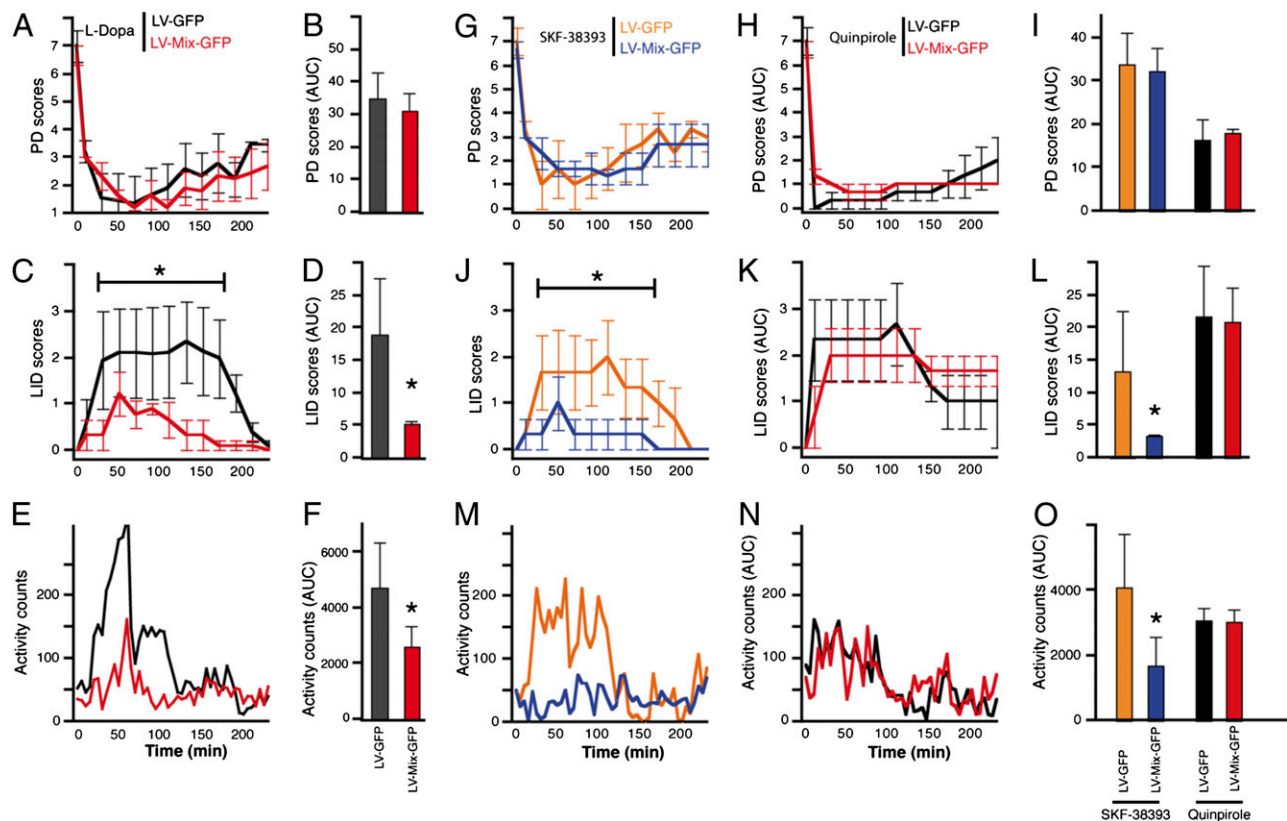
Fig. 4. LV-Mix-GFP expression in the macaque motor striatum reduces the dyskinesia elicited by L-dopa (*A–F*) and D1 and D2 agonists (*G–O*). Time-course panels reporting clinical ratings feature median scores ± SEM, but those reporting activity counts are shown without SEM for readability. Administration of L-dopa (levodopa/carbidopa 4:1, see *Materials and Methods*) or dopamine agonists starts at t = 0 min. (*A*) LV-Mix-GFP expression had no impact on the L-dopa–induced PD score at any time point. (*B*) The analysis of the area under the curve (AUC) of PD scores confirms this lack of effect (mean ± SEM). (*C*) LV-Mix-GFP expression reduced LID from t = 40 to t =160 min (but note peak at t = 50 min) in comparison with the LV-GFP animals (median scores; Mann–Whitney test, *$P < 0.05$). (*D*) The overall positive effect on LID severity is demonstrated further by the AUC data (mean ± SEM; unpaired *t* test; *$P < 0.05$). (*E* and *F*) Consequently, locomotor activity was lower in LV-Mix-GFP animals (mean ± SEM; unpaired *t* test; *$P < 0.05$). (*G–O*) Effects of D1 and D2 agonists in LV-Mix-GFP and LV-GFP monkeys were analyzed separately. (*G–I*) As with L-dopa, the antiparkinsonian effect of both (*G*) SKF-38393 (D1 agonist; 1.5 mg/kg, s.c.) and (*H*) quinpirole (D2 agonist; 1.5 mg/kg, s.c.) was comparable in both groups. (*J* and *K*) Although the severity of dyskinesia was comparable in both groups after administration of the D2 agonist (*K*), the LV-Mix-GFP animals displayed a reduced severity of D1 agonist-induced dyskinesia from t = 40 min to t = 160 min (*J*) (median scores; Mann–Whitney test; *$P < 0.05$). (*I*) AUC analysis supports this conclusion, showing that only the severity of dyskinesia induced by the D1 agonist is reduced more significantly in LV-Mix-GFP animals than in GFP animals (unpaired *t* test; *$P < 0.05$). (*M–O*) Analysis of the AUC of activity counts further supports the D1 agonist-mediated reduction in dyskinesia severity, because activity counts are significantly reduced in the LV-Mix-GFP animals compared with the GFP animals only after D1 agonist administration (unpaired *t* test; *$P < 0.05$).

a therapy to the brain would solve the problem only partially, because neuronal apoptosis may occur if the inhibition of the pathway exceeds a critical value (16, 17). Our work paves the way for an effective treatment of LID by targeting Ras-GRF1. This molecule is expressed exclusively in neurons of the CNS, and, more importantly, it is not linked to cell-survival pathways because it operates as a signaling integrator downstream of glutamate- and dopamine-mediated signals (18), which are dysregulated in LID (1–4). In addition, unlike observations for other ERK regulators (27), the absolute amount of the Ras-GRF1 proteins does not change in dyskinetic animals, making this molecule an appealing drug target because the efficacy of a Ras-GRF1–specific treatment would not be diminished by a compensatory elevation of its expression.

Our proof-of-concept study in the mouse shows that Ras-GRF1 deficiency can prevent the development of LID, possibly delaying its onset. Considering that the large majority (>80%) of PD patients will develop LID within 5–10 y from the initiation of dopaminergic drug therapy, the possibility of coadministering drugs acting on Ras-GRF1 as add-on agents appears to be a promising approach. Importantly, our data suggest that the combined administration of suboptimal doses of drugs acting on the MEK–ERK core component (such as SL327) may further enhance the antidyskinetic effect of Ras-GRF1 inhibition. This detail is a highly

relevant from a translational perspective. Indeed, many drugs targeting ERK are being developed for cancer therapy, and, although these drugs may have some systemic toxicity, they could be used at low doses, together with interventions targeting Ras-GRF1, to obtain an effective and safe treatment for LID.

Our data indicate that Ras-GRF1 is implicated not only in the dyskinesia-priming process but also in the expression of dyskinetic movements when LID is already established. Indeed, in the NHP model of LID, striatal inhibition of Ras-GRF1 and ERK signaling using viral vectors greatly ameliorated already established dyskinetic symptoms without affecting the therapeutic action of L-dopa.

Our work opens the way for a possible indication of gene therapy in PD, namely lentiviral-mediated delivery of signaling modulators that can "rebalance" the response of striatal neurons to L-dopa, thus controlling troublesome side effects without affecting the treatment's efficacy. A valid therapy based on Ras–ERK inhibition ought not to block this signaling pathway completely but only should reduce its abnormally high activation. Our results indicate that such a goal can be achieved by targeting Ras-GRF1. In addition, our work suggests that a therapy combining Ras-GRF1 partial inhibition with treatments affecting other signaling pathways may provide a more effective anti-dyskinetic approach with a low risk of untoward effects.

Materials and Methods

A detailed description of all materials and methods can be found in *SI Materials and Methods*. Briefly, generation of Ras-GRF1–KO mice has been described in refs. 18 and 19. Mice were injected with 1 μL of 6-OHDA-HCl (3 μg/μL) into the right medial forebrain bundle. 6-OHDA lesion surgery and behavioral testing were performed as previously described (22). Immunohistochemistry was carried out according to published procedures (9, 18, 42). The lentiviral vector expressing ERK2^{K52R} mutant has been described already (32). The two dominant-negative constructs, Ras-GRF1-NR2B-BD and Ras-GRF1-CD^{W1056E}, have been designed using the human Ras-GRF1 sequence and adapted from the mouse and rat sequences (30, 31).

Induction of parkinsonism and dyskinesia in NHP was performed as described in refs. 43 and 44. Lentiviral delivery surgery was performed using a convection-enhanced delivery method (43, 45) with a 1:1:1 mixture of the three vectors previously validated in the mouse. Starting at 8 wk postsurgery, animals were examined every 2 d for behavioral responses to their tailored dose of L-dopa, the D1 agonist SKF-38393 (1.5 mg/kg, s.c.), or the D2/D3 agonist quinpirole (1.5 mg/kg, s.c.) (46). Postmortem processing was carried out as described (47).

1. Jenner P (2008) Molecular mechanisms of L-DOPA-induced dyskinesia. *Nat Rev Neurosci* 9:665–677.
2. Cenci MA (2007) Dopamine dysregulation of movement control in L-DOPA-induced dyskinesia. *Trends Neurosci* 30:236–243.
3. Calabresi P, Di Filippo M, Ghiglieri V, Picconi B (2008) Molecular mechanisms underlying levodopa-induced dyskinesia. *Mov Disord* 23(Suppl 3):S570–S579.
4. Cenci MA, Lundblad M (2006) Post- versus presynaptic plasticity in L-DOPA-induced dyskinesia. *J Neurochem* 99:381–392.
5. Orban PC, Chapman PF, Brambilla R (1999) Is the Ras-MAPK signalling pathway necessary for long-term memory formation? *Trends Neurosci* 22:38–44.
6. Fasano S, Brambilla R (2002) Cellular mechanisms of striatum-dependent behavioral plasticity and drug addiction. *Curr Mol Med* 2:649–665.
7. Brambilla R (2003) Targeting Ras/ERK signaling in the striatum: Will it help? *Mol Psychiatry* 8:366–368.
8. Girault JA, Valjent E, Caboche J, Hervé D (2007) ERK2: A logical and gate critical for drug-induced plasticity? *Curr Opin Pharmacol* 7:77–85.
9. Westin JE, Vercammen L, Strome EM, Konradi C, Cenci MA (2007) Spatiotemporal pattern of striatal ERK1/2 phosphorylation in a rat model of L-DOPA-induced dyskinesia and the role of dopamine D1 receptors. *Biol Psychiatry* 62:800–810.
10. Santini E, et al. (2007) Critical involvement of cAMP/DARPP-32 and extracellular signal-regulated protein kinase signaling in L-DOPA-induced dyskinesia. *J Neurosci* 27:6995–7005.
11. Pavón N, Martín AB, Mendialdua A, Moratalla R (2006) ERK phosphorylation and FosB expression are associated with L-DOPA-induced dyskinesia in hemiparkinsonian mice. *Biol Psychiatry* 59:64–74.
12. Schuster S, et al. (2008) The 3-hydroxy-3-methylglutaryl-CoA reductase inhibitor lovastatin reduces severity of L-DOPA-induced abnormal involuntary movements in experimental Parkinson's disease. *J Neurosci* 28:4311–4316.
13. Sweatt JD (2001) The neuronal MAP kinase cascade: A biochemical signal integration system subserving synaptic plasticity and memory. *J Neurochem* 76:1–10.
14. Davis S, Laroche S (2006) Mitogen-activated protein kinase/extracellular regulated kinase signalling and memory stabilization: A review. *Genes Brain Behav* 5(Suppl 2):61–72.
15. Ramos JW (2008) The regulation of extracellular signal-regulated kinase (ERK) in mammalian cells. *Int J Biochem Cell Biol* 40:2707–2719.
16. Cagnol S, Chambard JC (2010) ERK and cell death: Mechanisms of ERK-induced cell death—apoptosis, autophagy and senescence. *FEBS J* 277:2–21.
17. Kim EK, Choi EJ (2010) Pathological roles of MAPK signaling pathways in human diseases. *Biochim Biophys Acta* 1802:396–405.
18. Fasano S, et al. (2009) Ras-guanine nucleotide-releasing factor 1 (Ras-GRF1) controls activation of extracellular signal-regulated kinase (ERK) signaling in the striatum and long-term behavioral responses to cocaine. *Biol Psychiatry* 66(8):758–768.
19. Brambilla R, et al. (1997) A role for the Ras signalling pathway in synaptic transmission and long-term memory. *Nature* 390:281–286.
20. Lundblad M, et al. (2005) Pharmacological validation of a mouse model of l-DOPA-induced dyskinesia. *Exp Neurol* 194:66–75.
21. Darmopil S, Martín AB, De Diego IR, Ares S, Moratalla R (2009) Genetic inactivation of dopamine D1 but not D2 receptors inhibits L-DOPA-induced dyskinesia and histone activation. *Biol Psychiatry* 66:603–613.
22. Lundblad M, Picconi B, Lindgren H, Cenci MA (2004) A model of L-DOPA-induced dyskinesia in 6-hydroxydopamine lesioned mice: Relation to motor and cellular parameters of nigrostriatal function. *Neurobiol Dis* 16:110–123.
23. Valjent E, et al. (2000) Involvement of the extracellular signal-regulated kinase cascade for cocaine-rewarding properties. *J Neurosci* 20:8701–8709.
24. Santini E, et al. (2009) L-DOPA activates ERK signaling and phosphorylates histone H3 in the striatonigral medium spiny neurons of hemiparkinsonian mice. *J Neurochem* 108:621–633.
25. Konradi C, et al. (2004) Transcriptome analysis in a rat model of L-DOPA-induced dyskinesia. *Neurobiol Dis* 17:219–236.
26. Valastro B, et al. (2007) Proteomic analysis of striatal proteins in the rat model of L-DOPA-induced dyskinesia. *J Neurochem* 102:1395–1409.
27. Crittenden JR, et al. (2009) Dysregulation of CalDAG-GEFI and CalDAG-GEFII predicts the severity of motor side-effects induced by anti-parkinsonian therapy. *Proc Natl Acad Sci USA* 106:2892–2896.
28. Amendola M, Venneri MA, Biffi A, Vigna E, Naldini L (2005) Coordinate dual-gene transgenesis by lentiviral vectors carrying synthetic bidirectional promoters. *Nat Biotechnol* 23:108–116.
29. Indrigo M, Papale A, Orellana D, Brambilla R (2010) Lentiviral vectors to study the differential function of ERK1 and ERK2 MAP kinases. *Methods Mol Biol* 661:205–220.
30. Krapivinsky G, et al. (2003) The NMDA receptor is coupled to the ERK pathway by a direct interaction between NR2B and RasGRF1. *Neuron* 40:775–784.
31. Vanoni M, et al. (1999) Characterization and properties of dominant-negative mutants of the ras-specific guanine nucleotide exchange factor CDC25(Mm). *J Biol Chem* 274:36656–36662.
32. Vantaggiato C, et al. (2006) ERK1 and ERK2 mitogen-activated protein kinases affect Ras-dependent cell signaling differentially. *J Biol* 5:14.1–14.15.
33. Stocchi F, Tagliati M, Olanow CW (2008) Treatment of levodopa-induced motor complications. *Mov Disord* 23(Suppl 3):S599–S612.
34. Buck K, Ferger B (2010) L-DOPA-induced dyskinesia in Parkinson's disease: A drug discovery perspective. *Drug Discov Today* 15(19-20):867–875.
35. Bateup HS, et al. (2010) Distinct subclasses of medium spiny neurons differentially regulate striatal motor behaviors. *Proc Natl Acad Sci USA* 107:14845–14850.
36. Ahmed MR, et al. (2010) Lentiviral overexpression of GRK6 alleviates L-dopa-induced dyskinesia in experimental Parkinson's disease. *Sci Transl Med* 2(28):28ra28.
37. Cenci MA, Konradi C (2010) Maladaptive striatal plasticity in L-DOPA-induced dyskinesia. *Prog Brain Res* 183:209–233.
38. Isacson O, Kordower JH (2008) Future of cell and gene therapies for Parkinson's disease. *Ann Neurol* 64(Suppl 2):S122–S138.
39. Lundberg C, et al. (2008) Applications of lentiviral vectors for biology and gene therapy of neurological disorders. *Curr Gene Ther* 8:461–473.
40. Nanou A, Azzouz M (2009) Gene therapy for neurodegenerative diseases based on lentiviral vectors. *Prog Brain Res* 175:187–200.
41. Ramaswamy S, Soderstrom KE, Kordower JH (2009) Trophic factors therapy in Parkinson's disease. *Prog Brain Res* 175:201–216.
42. Andersson M, Konradi C, Cenci MA (2001) cAMP response element-binding protein is required for dopamine-dependent gene expression in the intact but not the dopamine-denervated striatum. *J Neurosci* 21:9930–9943.
43. Berton O, et al. (2009) Striatal overexpression of DeltaJunD resets L-DOPA-induced dyskinesia in a primate model of Parkinson disease. *Biol Psychiatry* 66:554–561.
44. Bézard E, et al. (2003) Attenuation of levodopa-induced dyskinesia by normalizing dopamine D3 receptor function. *Nat Med* 9:762–767.
45. Gold SJ, et al. (2007) RGS9-2 negatively modulates L-3,4-dihydroxyphenylalanine-induced dyskinesia in experimental Parkinson's disease. *J Neurosci* 27:14338–14348.
46. Boraud T, Bezard E, Bioulac B, Gross CE (2001) Dopamine agonist-induced dyskinesias are correlated to both firing pattern and frequency alterations of pallidal neurones in the MPTP-treated monkey. *Brain* 124:546–557.
47. Guigoni C, et al. (2005) Levodopa-induced dyskinesia in MPTP-treated macaques is not dependent on the extent and pattern of nigrostrial lesioning. *Eur J Neurosci* 22:283–287.

NEUROSCIENCE